The use of neutron reflectivity in determining the structure of a platinum - carbon multi-layer

1996 J. Phys.: Condens. Matter 8 4115

(http://iopscience.iop.org/0953-8984/8/23/004)

J. Phys.: Condens. Matter **8** (1996) 4115–4124. Printed in the UK

The use of neutron reflectivity in determining the structure of a platinum–carbon multi-layer

N M Harwood†, S Messoloras‡ and R J Stewart†

† J J Thomson Physical Laboratory, University of Reading, Whiteknights, PO Box 220, Reading RG6 6AF, UK

‡ The University of Athens, Physics Department, Solid State Section, Panepistimiopolis, Zografos, Athens GR 157 84, Greece

Received 4 September 1995, in final form 16 February 1996

Abstract. The neutron reflectivity from three platinum–carbon bilayers on a silicon substrate has been measured using θ–2θ scans. The thicknesses and densities of the layers are determined and also the nature of the multi-layer–substrate interface is deduced. This is accomplished by modelling the reflectivities of different multi-layer structures and comparing them to the experimental data.

1. Introduction

In recent years there has been considerable interest in materials which have low-dimensional structures. These materials have physical properties which differ from those of the bulk due to a small structure scale in at least one direction. Multi-layers can be grown by sequentially depositing many layers of different materials onto a substrate. Such materials provide a new generation of electronic and optical devices, for example, multiple-quantum-well lasers. Multi-layer stacks of alternate layers of a continuous metal film (e.g. Pt) and a spacer element (e.g. C) which form a periodic structure (PtCPtCPtC. . .) behave as a pseudo-crystal (Xu and Evans 1991). Such stacks can be used as a mirror to (Bragg) reflect soft x-rays. Pt–C multilayers have a high x-ray reflectivity because of their large refractive index difference for x-rays, and have been used as soft-x-ray mirrors in space and laser plasma experiments (Evans *et al* 1994). Such mirrors are currently limited to the soft-x-ray region since the thinner layer periodicities required for shorter wavelengths cannot be produced with sufficient quality. Interdiffusion between layers and surface and interfacial irregularities are the major problems in multi-layer materials and it is crucially important to be able to monitor these effects and their influence on the physical properties of devices using such multi-layer stacks.

Long-wavelength neutron reflectivity measurements provide a useful non-destructive technique for the measurement of the overall structure and the interfacial irregularities present in such thin-film structures. The reflectivity is measured over a range of momentum transfers which is determined by both the angle of the sample with respect to the incident beam and the neutron wavelength. An experiment is carried out at either variable wavelength using the time of flight (TOF) technique or at variable angle (θ–2θ scans). In this study θ–2θ scans were used to measure the reflectivity of a Pt–C multi-layer using the D17 small-angle neutron scattering instrument at the Institut Laue–Langevin, Grenoble, France.

0953-8984/96/234115+10$19.50

The purpose of this work is to measure the thicknesses and densities of the layers and to determine information about any surface or interfacial irregularities present. In addition it intends to show that the neutron reflectivity technique can contribute significantly in the structural characterization of multi-layer structures and detailed information can be obtained by a full analysis of the results.

2. Theory

At small glancing angles the neutron interacts with the bulk rather than the individual nuclei. In a manner similar to conventional optics we can define an index of refraction, n, which depends only on the average potential which the neutron experiences in the medium and is independent of the actual atomic structure. For neutrons, n is close to unity and is given by (Goldberger and Seitz 1947)

$$n = 1 - \lambda^2 \rho / 2\pi \qquad \rho = \sum_i N_i \langle b_i \rangle \tag{1}$$

where λ is the incident neutron wavelength, N_i is the number of atoms per unit volume of species i and $\langle b_i \rangle$ is the mean scattering length for species i.

The reflectivity is calculated by using the continuity of the neutron wave function and its first derivative at the boundary between neighbouring media and equations similar to those of conventional optics apply (Born and Wolf 1969). For angles lower than a critical angle, α_c, the reflectivity is one (total reflection). For a multi-layer, the application of the continuity equations at each interface leads to an expression for each layer which can be written in matrix form as

$$M_j = \begin{bmatrix} \cos\Delta_j & (-\mathrm{i}/P_j)\sin\Delta_j \\ -\mathrm{i}P_j \sin\Delta_j & \cos\Delta_j \end{bmatrix} \tag{2}$$

$$\Delta_j = (2\pi/\lambda) n_j d_j \sin\alpha_j \qquad P_j = n_j \sin\alpha_j$$

where α_j is the glancing angle at the interface of the jth and $(j+1)$th layers and n_j is the refractive index of the jth layer and d_j its thickness. The matrix is completely characteristic of the properties of the jth layer. Simple matrix multiplication gives the resultant effect of m such layers as

$$M = [M_1] \ldots [M_m] = \begin{bmatrix} M_{11} & M_{12} \\ M_{21} & M_{22} \end{bmatrix} \tag{3}$$

The reflectivity is then given by $R = rr^*$ where

$$r = [P_0(M_{11} + P_s M_{12}) - (M_{21} + M_{22} P_s)]/[P_0(M_{11} + P_s M_{12}) + (M_{21} + M_{22} P_s)]. \tag{4}$$

The index zero represents the first medium (air) and s is the substrate. In order to calculate the angles we use Snell's law, $n_0 \cos\alpha_0 = n_1 \cos\alpha_1 = \cdots = n_j \cos\alpha_j = \cdots = n_s \cos\alpha_s$. This method is suitable for computer implementation and the reflectivity of any multi-layer system can be calculated and compared to the measured reflectivity. The curves obtained are plotted as a function of the magnitude of the scattering vector, Q, where $|Q| = 4\pi \sin\alpha/\lambda$. Interference terms are observed and the position of the mth order fringe is given by

$$(Q_m^2 - Q_c^2) \cong (2\pi m / D^2) \tag{5}$$

where c refers to the critical angle and D is the total thickness of the multi-layer stack. The separation of the fringes, therefore, gives a value for the thickness of a single layer or in

this case the total thickness of a multi-layer. The average scattering length density of the multi-layer can be determined from the critical angle where

$$Q_c \approx 4(\pi \langle \rho \rangle)^{1/2}. \tag{6}$$

For a system of bilayers there will be a series of Bragg peaks superimposed on top of the interference fringes; the position of the first Bragg peak, Q_B, can be used to determine the average bilayer thickness, d, using $Q_B = 2\pi/d$ (Saxena and Shoenborn 1977). The reflectivity of this first Bragg peak is given by (Sears 1983)

$$R_B = 4N^2 d^4 (\rho_1 - \rho_2)^2/\pi^2 \tag{7}$$

where N is the number of bilayers. In the case of a multi-layer having non-sharp interfaces, where interdiffusion of atoms from one layer to another has occurred, the interface can be split up into many thin layers and the resultant reflectivity calculated.

3. Results and discussion

The sample used in this experiment consisted of three Pt–C bilayers with an extra Pt layer at the top, deposited by ion beam sputtering on an Si substrate; each layer was nominally 3 nm thick. The reflectivity measurements were made on the D17 spectrometer at the I.L.L., using a constant wavelength of 1.2 nm and variable angle, giving a Q range of between 0.1 and 1.5 nm^{-1} (θ–2θ scans). An apparatus utilizing a stepper motor, shaft encoder and driver/reader logic was used in order to rotate the multi-layer sample in the neutron beam with positioning accuracy of 0.1 mrad. The angular divergence ($\Delta\theta/\theta$) of the experiment is defined by the surface area of the sample onto which the beam is incident rather than the collimating apertures. Since $\Delta\theta/\theta$ is small the overall resolution is defined by the wavelength resolution (4%). The data were corrected for air scattering (measurements without a sample in the beam), for detector efficiency and for the different beam area cut by the sample as its angle to the incident beam changed.

The data were modelled by reflectivity curves computed using the matrix formulation described above. In the calculated reflectivities a nominal resolution effect has been introduced in order to remove the sharpness of the minima. The appropriate resolution is fitted to the final model. For all the simulations discussed here the substrate density is assumed constant at that of crystalline silicon, which corresponds to a scattering length density of $\rho_{Si} = 2.15 \times 10^{-4}$ nm^{-2}.

From the position of the interference fringes the total thickness of the multi-layer structure has been calculated as 26.6 nm. This total thickness, assuming that all seven layers have the same thickness, corresponds to a thickness of 3.8 nm for each layer. In order to simulate the reflectivity from this structure we assume that the densities of Pt and C are 21.4 and 2.0 g cm^{-3}, respectively, which corresponds to scattering length densities of $\rho_{Pt} = 6.3 \times 10^{-4}$ nm^{-2} and $\rho_C = 6.6 \times 10^{-4}$ nm^{-2} (calculated from the known b for C and Pt). Further we will initially assume that all the interfaces are sharp. A comparison between the experimental data and a model of the multi-layer structure described above is shown in figure 1 (curve a). It can be seen that there is poor agreement between the simulation and the experimental data. It is clear that, because the critical angle is offset by an amount far larger than the sample positioning error (0.01 nm^{-1}), the average scattering length density of the multi-layer is higher than that used in the model (6). The multi-layer thickness appears to be approximately correct, as the higher-order fringes between the experimental data and the simulation are in reasonable agreement (equation (5)). However, the first-order peak in the experimental data is at lower Q in comparison with the simulated curve and the second

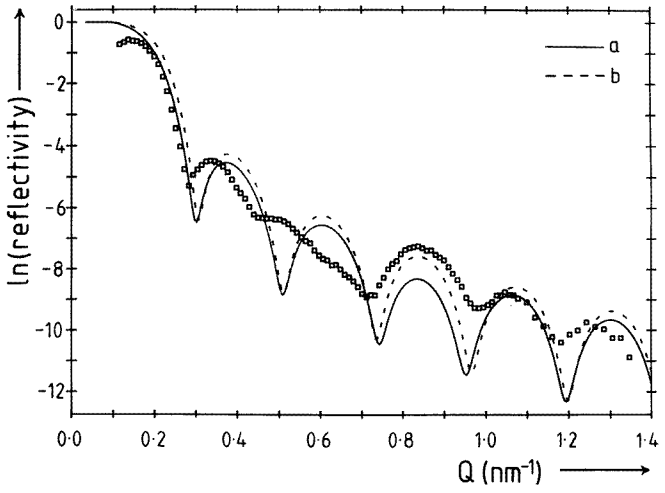

Figure 1. A comparison of the experimental data (points) and the calculated reflectivities from layers with sharp interfaces. Curve a, three Pt–C bilayers plus one Pt layer all of the same thickness on an Si substrate ($d_{layer} = 3.8$ nm, $\rho_{Pt} = 6.3\times10^{-4}$ nm^{-2}, $\rho_C = 6.6\times10^{-4}$ nm^{-2}). Curve b, a single layer of thickness 26.6 nm and $\langle\rho\rangle = 7.2\times10^{-4}$ nm^{-2}.

peak has been flattened out into a shoulder and shows signs of splitting into more than one fringe.

From (6) and the experimental value of Q_c we obtain an average scattering length density of $\langle\rho\rangle = 7.2\times10^{-4}$ nm^{-2} which is higher than the average value of $\langle\rho\rangle = 6.45\times10^{-4}$ nm^{-2} used in the simulation (curve a, figure 1). In order to examine whether the average scattering length density calculated above fits the experimental data better, the reflectivity of a single layer of thickness 26.6 nm and $\rho = 7.2\times10^{-4}$ nm^{-2} is also presented in figure 1 (curve b). This new curve fits the rate of fall of the experimental data better, thus determining the approximate value for the average scattering length density of the multi-layer.

Having obtained an approximate value for the average scattering length density the contrast between the scattering length densities of the layers has to be determined. The overall thickness of the multi-layer was found to be 26.6 nm, thus the corresponding bilayer thickness would be 7.6 nm (if all the layers are of equal thickness). If this bilayer thickness is used the first Bragg peak is calculated to be at $Q = 0.83$ nm^{-1} ($Q = 2\pi/d$). The reflectivity arising from the Bragg peak is given by (7) which shows that its magnitude depends on the difference between the scattering length densities of the Pt and C layers. Thus, by fitting the Bragg peak the scattering length density of the individual layers can be determined. In figure 2 the effect of different scattering length densities for the Pt and C layers is examined, keeping the average ρ constant (at 7.2×10^{-4} nm^{-2}) and the thickness of each layer as 3.8 nm. If the scattering length density of the Pt layers is increased by 8% above the average ρ and that of the C layers correspondingly reduced, the Bragg peak becomes more prominent (figure 2, curve a). If we reverse the situation (Pt layers decreased by 8% and C layers increased) the Bragg peak decreases in size and is now smaller than the interference fringes (figure 2, curve b). In a more extreme situation of a 12% decrease in the Pt level and a corresponding increase in the C level the Bragg peak turns into a trough (figure 2, curve c); this effect is caused by the extra Pt layer. The best fit to the Bragg peak is obtained by the scattering length densities of $\rho_{Pt} = 7.8\times10^{-4}$ nm^{-2} and

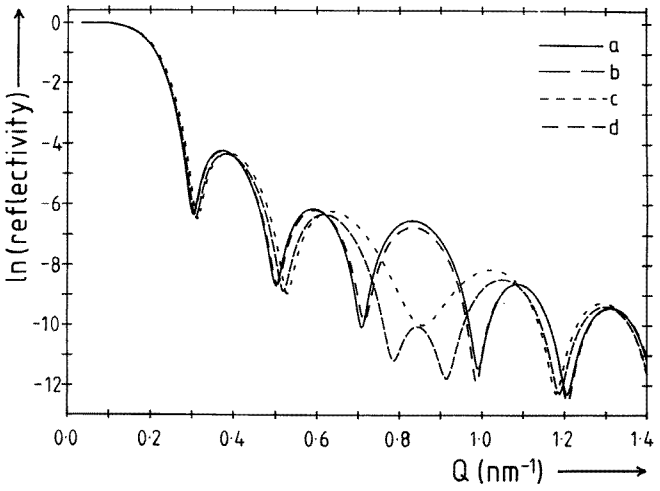

Figure 2. The effect of varying the scattering length densities of the individual layers whilst keeping the average scattering length density of the three Pt–C bilayers plus one Pt layer constant; $d_{layer} = 3.8$ nm. Curve a, $\rho_{Pt} = 7.8 \times 10^{-4}$ nm^{-2}, $\rho_C = 6.6 \times 10^{-4}$ nm^{-2}; curve b, $\rho_{Pt} = 6.6 \times 10^{-4}$ nm^{-2}, $\rho_C = 7.8 \times 10^{-4}$ nm^{-2}; curve c, $\rho_{Pt} = 6.3 \times 10^{-4}$ nm^{-2}, $\rho_C = 8.1 \times 10^{-4}$ nm^{-2}; curve d, sinusoidal variation of the scattering length density with maximum value 7.8×10^{-4} nm^{-2} and minimum value 6.6×10^{-4} nm^{-2} and a half period of 3.8 nm.

$\rho_C = 6.6 \times 10^{-4}$ nm^{-2} (figure 2 curve a).

We now investigate the effect of any interfacial irregularities between the Pt and C layers. The extreme case of a sinusoidal variation in the scattering length density of the layers is also shown in figure 2 (curve d). Peak values of 7.8×10^{-4} nm^{-2} for the Pt and 6.6×10^{-4} nm^{-2} for the C layers are assumed with a period of 7.6 nm (the same as the bilayer thickness). The resulting reflectivity shows remarkably little difference from the equivalent model curve for the multi-layer with sharp interfaces (curve a), the only significant change being a slight decrease in the Bragg peak intensity, which is predicted by the kinematic theory (Saxena and Shoenborn 1977). Thus, little information can be obtained about the nature of the inter-layer interfaces.

Large changes are often produced in the reflectivity by non-sharp air–layer and layer–substrate interfaces (Harwood *et al* 1988). The form of these interfaces will now be considered in order to obtain a better fit of the first two interference fringes of the experimental data. The model in figure 2 (curve a) with layers of thickness 3.8 nm and $\rho_{Pt} = 7.8 \times 10^{-4}$ nm^{-2}, $\rho_C = 6.6 \times 10^{-4}$ nm^{-2} is used as a marker for comparison with the other models. Firstly, a Gaussian shaped layer–substrate interface is modelled, starting the interface profile at the level of the last Pt layer and finishing at that for Si. A wide interface of total width 20 nm produces a pronounced effect on the reflectivity (figure 3, curve b). The first two peaks have moved to lower Q values agreeing better with the experimental data. However, the Bragg peak is broadened and the last two fringes are decreased in amplitude and shifted to higher Q values. If the interface is doubled in thickness to 40 nm, the first two oscillations are severely flattened out (curve c) and to a greater extent than the experimental data. Also shown in figure 3 (curve d) is a model of a 16 nm thick interface, but starting at a lower ρ value than that of curves b and c. This interface represents the possible diffusion of C from the sixth layer through the last Pt layer and into the substrate.

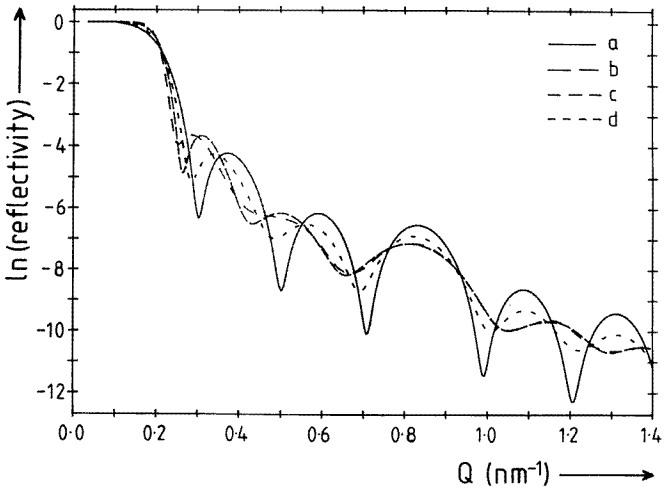

Figure 3. The effect of a non-sharp layer–substrate interface on the calculated reflectivities for three Pt–C bilayers plus one Pt layer on an Si substrate, $d_{layer} = 3.8$ nm, $\rho_{Pt} = 7.8\times10^{-4}$ nm^{-2}, $\rho_C = 6.6 \times 10^{-4}$ nm^{-2}. Curve a, sharp layer–substrate interface. Curve b, 20 nm interface starting at $\rho = 7.8 \times 10^{-4}$ nm^{-2}. Curve c, 40 nm interface starting at $\rho = 7.8 \times 10^{-4}$ nm^{-2}. Curve d, 16 nm interface starting at $\rho = 5.6 \times 10^{-4}$ nm^{-2}.

In this last simulation the first two fringes have again moved to lower Q values, whilst the higher-order Q fringes remain in the same position as for curve a.

In the case of a non-sharp air–layer interface, which might have been caused by surface contamination, similar shifts in the position of the fringes as noted for the non-sharp layer–substrate interface are produced as shown in figure 4 (curve b). An improved fit is not, however, obtained because the reflectivity falls off faster than before (curve a). This effect is similar to surface roughness which can be approximated by an exponential modification term (Braslau *et al* 1985, Nevot and Croce 1980). It is also possible that effects such as surface oxidation may increase the scattering length density at the air–multi-layer interface (Ashworth *et al* 1989). This effect is also shown in figure 4 (curve c) and results in an increase of the overall level of the reflectivity; this will give an improved fit to the data.

Other effects can be modelled, for instance, if one layer is made thicker than the others, whilst the overall multi-layer thickness is kept constant. This is shown in figure 5 (curve b) where one layer (the C layer nearest to the substrate) is doubled in thickness to 7.4 nm and the other layers are reduced to 3.2 nm.

The best fit to the experimental data, using the above modelling is shown in figure 6. This simulation assumes four Pt layers, each of thickness 3.6 nm, and three C layers, two of thickness 3.6 nm and one of 5.0 nm, the total width of the multi-layer being 26.6 nm (excluding the width of the layer–substrate interface). Scattering length densities are $\rho_{Pt} = 7.8\times10^{-4}$nm^{-2}, $\rho_C = 6.6\times10^{-4}$ nm^{-2} and $\rho_{Si} = 2.15\times10^{-4}$ nm^{-2} with the first Pt layer scattering length density increased at the surface (1.8 nm) to 9.5×10^{-4} nm^{-2}. The layer–substrate interface is a 15 nm Gaussian distribution starting at 5.6×10^{-4} nm^{-2}. This interface represents the diffusion of C through the last Pt layer and deep into the substrate.

There is still, however, a significant difference between the second interference fringe of the calculated reflectivity and the experimental data. In the experimental data this fringe has been flattened out and shows signs of splitting into two fringes. The best explanation

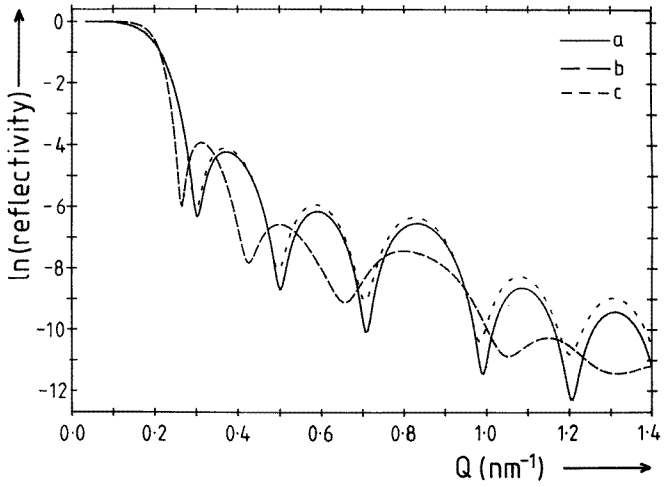

Figure 4. The effect of varying the air–layer interface on the calculated reflectivities for three Pt–C bilayers plus one Pt layer on an Si substrate, $d_{layer} = 3.8$ nm, $\rho_{Pt} = 7.8 \times 10^{-4}$ nm^{-2}, $\rho_C = 6.6 \times 10^{-4}$ nm^{-2}. Curve a, sharp air–layer interface. Curve b, 20 nm air–layer interface. Curve c, sharp air–layer interface plus a 1.8 nm surface layer of $\rho = 9.5 \times 10^{-4}$ nm^{-2}.

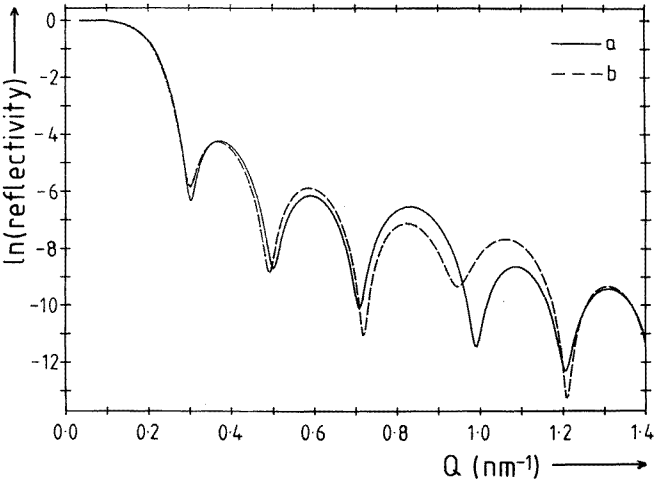

Figure 5. The effect on the calculated reflectivities of varying the individual layer thickness whilst keeping the total thickness = 26.6 nm for three Pt–C bilayers plus one Pt layer on an Si substrate. Curve a, $d_{layer} = 3.8$ nm, $\rho_{Pt} = 7.8 \times 10^{-4}$ nm^{-2}, $\rho_C = 6.6 \times 10^{-4}$ nm^{-2}. Curve b, $d_{layer} = 3.2$ nm for six layers and the C layer next to the substrate is of thickness 7.4 nm.

for this effect is that a second frequency is present in the experimental data. This is shown in figure 7 by modelling the reflectivity from just two layers, one of thickness 30 nm and scattering length density 7.8×10^{-4} nm^{-2} and the other of thickness 5.5 nm and scattering length density 5.0×10^{-4} nm^{-2}. This simulation gives good agreement with the first two fringes. If this profile for the layer–substrate interface is combined with the best fit of the data obtained previously (figure 6) a significantly better fit is obtained (figure 8). Further

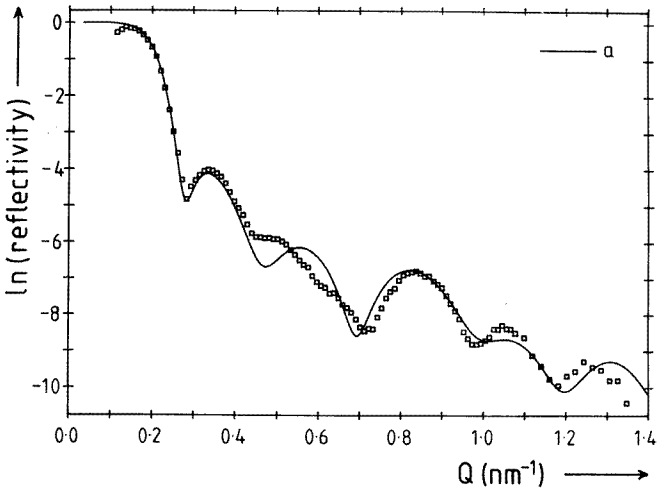

Figure 6. A comparison of the experimental data (points) and the best model fit (line) from the combined effects shown in figures 1–5. The calculated reflectivity is for three Pt–C bilayers plus one Pt layer on an Si substrate ($d_{layer} = 3.6$ nm, $\rho_{Pt} = 7.8\times10^{-4}$ nm^{-2}, $\rho_C = 6.6\times10^{-4}$ nm^{-2}, top Pt layer 5.0 nm plus a 1.8 nm surface layer of $\rho = 9.5 \times 10^{-4}$ nm^{-2}, and a 15 nm layer–substrate interface starting at $\rho = 5.6 \times 10^{-4}$ nm^{-2}).

in this final simulation the layers are of thickness 3.4 nm , with the exception of the C layer nearest to the substrate which has been doubled in thickness to 6.8 nm. Scattering length densities are as used in figure 6 ($\rho_{Pt} = 7.8 \times 10^{-4}$ nm^{-2}, $\rho_C = 6.6 \times 10^{-4}$ nm^{-2}). The first layer has an increased scattering length density at the surface. The layer–substrate interface consists of two parts, which could be attributed to the different diffusivities of Pt and C. The first part has a constant $\rho = 5.0 \times 10^{-4}$ nm^{-2} and is of width 5.5 nm, the second is of total width 2.0 nm and penetrates into the substrate. In this final fit a resolution effect of $\Delta Q/Q = 0.04$ has been implemented. This resolution is consistent with the experimental wavelength resolution (FWHM 4%) and shows that the angular beam divergence was insignificant as expected (the angular divergence is defined by the sample area projected to the beam).

4. Conclusions

The neutron reflectivity of a multi-layer consisting of three Pt–C bilayers plus one extra Pt layer on an Si substrate has been measured at constant wavelength, 1.2 nm, and variable angle of incidence. The overall thickness of the multi-layer is determined to be 26.6 nm which is equal to the nominal thickness. The individual layer thicknesses are deduced as 3.4 nm but one carbon layer has a thickness of 6.8 nm. The scattering length density of the Pt layers was found to be 7.8×10^{-4} nm^{-2} whilst that for the C layers was 6.6×10^{-4} nm^{-2}. The scattering length densities expected for Pt and C are 6.3×10^{-4} nm^{-2} and 6.6×10^{-4} nm^{-2}, respectively. This increase of the scattering length density of the Pt layers would imply either an increase in the Pt layer density (from 21.4 to 26.6 g cm^{-1}) or that C atoms diffuse to the Pt layers. The first possibility is unlikely, since it is difficult to envisage such a much higher density than that of the crystalline Pt. If carbon atoms diffuse into the Pt layers, a 13 at.% concentration of C in the Pt layers, possibly in interstitial positions, would explain

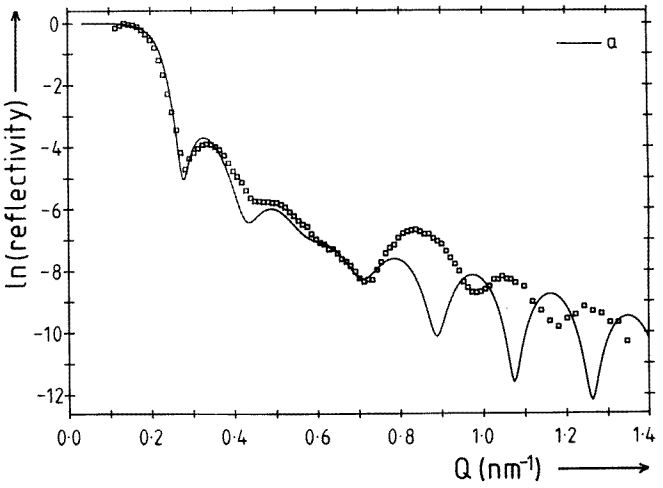

Figure 7. An attempt to fit the second interference peak in the experimental data (points). The line is the calculated reflectivity for two layers on an Si substrate, $\rho_1 = 7.8 \times 10^{-4}$ nm^{-2} and thickness 30.0 nm, $\rho_2 = 5.0 \times 10^{-4}$ nm^{-2} and thickness 5.5 nm (layer 2 is nearest to the substrate).

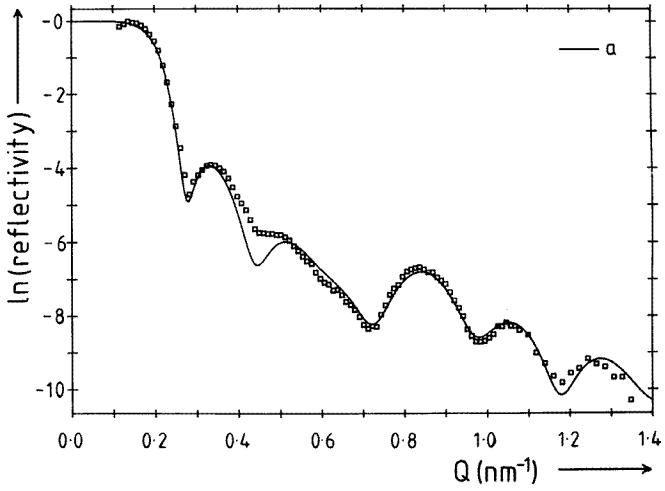

Figure 8. The final fit of the experimental data (points). The calculated reflectivity is for three Pt–C bilayers plus one Pt layer on an Si substrate ($d_{layer} = 3.4$ nm, $\rho_{Pt} = 7.8 \times 10^{-4}$ nm^{-2}, $\rho_C = 6.6 \times 10^{-4}$ nm^{-2}, sixth layer 6.8 nm plus a 1.8 nm surface layer of $\rho = 9.5 \times 10^{-4}$ nm^{-2}; the layer–substrate interface has two regions, one of width 5.5 nm and constant $\rho = 5.0 \times 10^{-4}$ nm^{-2}, the other a Gaussian of total width of 2 nm leading into the substrate).

the measured value of the scattering length density. The determined scattering length density of carbon corresponds to a density of $d = 2.0$ g cm^{-3} which is similar to that expected for amorphous carbon (d in the range 1.8–2.1 g cm^{-3}).

A wide interface between the multi-layer and the substrate is deduced, having a total

width of 7.5 nm. This interface is described by two characteristic lengths: 5.5 nm of constant scattering length density and a Gaussian tail of 2 nm. This implies that C and Pt atoms have diffused into the substrate but to different depths, the C atoms being more mobile, penetrating through the last Pt layer and deep into the substrate.

Thus using neutron reflectivity, detailed information about the layer thicknesses, interfacial irregularities and interdiffusion has been deduced. Many properties of the multi-layers depend on the interface (e.g. scattering of conduction electrons) and the detailed structural information on the interface provided by neutron reflectivity is important is constructing theoretical models in order to explain other types of measurement. For many applications or for the understanding of their physical properties, low-dimensional structures with sharp interfaces and as little interdiffusion as possible are required. Improvements in the quality of the fabricated structures can be obtained by controlling different growth parameters (e.g. gas pressure, ion gun current and voltage and substrate temperature). The effect which these different growth parameters have on the quality of the multi-layer structures can be unambiguously determined by neutron reflectivity and thus an appropriate choice of growth conditions can be made. In addition neutron reflectivity can be used as a quality control of industrially grown multi-layers for different applications.

Acknowledgments

We are indebted to Dr B L Evans of the University of Reading, Physics Department for preparing the sample used in this experiment. One of us (NMH) would like to thank the EPSRC for a postgraduate studentship. The experiments were carried out at the Institute Laue–Langevin, Grenoble, France and we would like to thank the EPSRC for their financial support in enabling us to carry out the experiments.

References

Ashworth C D, Messoloras S, Stewart R J and Penfold J 1989 *Semicond. Sci. Technol.* **4** 1
Born M and Wolf E 1969 *Principles of Optics* (Oxford: Pergamon)
Braslau A, Deutsch M, Pershan P S, Weiss A H, Als-Nielsen J and Bohr J 1985 *Phys. Rev. Lett.* **54** 114
Evans B L, Maaroof A I and Xu S 1994 *J. Appl. Phys.* **76** 900
Goldberger M L and Seitz F 1947 *Phys. Rev.* **71** 294
Harwood N M, Messoloras S, Stewart R J, Penfold J and Ward R C 1988 *Phil. Mag.* B **2** 217
Nevot L and Croce P 1980 *Rev. Phys. Appl.* **15** 761
Saxena A M and Shoenborn B P 1977 *Acta Crystallogr.* A **33** 805
Sears V F 1983 *Acta Crystallogr.* A **39** 601
Xu S and Evans B L 1991 *J. Mod. Opt.* **38** 1631